$^{37}Cl(p,n)^{37}Ar$ excitation function up to 24 MeV: Study of (p,n) reactions*

R. Kishore,† R. Collé,‡ S. Katcoff, and J. B. Cumming
Chemistry Department, Brookhaven National Laboratory, Upton, New York 11973
(Received 17 June 1974; revised manuscript received 10 February 1975)

Cross sections for the $^{37}Cl(p,n)^{37}Ar$ reaction were determined from 2 to 24 MeV by the activation method. NaCl targets of natural isotopic composition were irradiated inside of Al cells having thin Havar windows. Beam intensities were determined with a Faraday cup and the ^{37}Ar disintegration rates were measured with internal gas proportional counters. The cross sections (±6% uncertainty) increase from threshold (1.64 MeV) to a broad maximum of 365 mb at 10 MeV and then decrease to 34 mb at 23.5 MeV. These results and five other recently measured (p,n) excitation functions are compared with each other and with various cascade-evaporation calculations. Reasonable agreement was attained between experiment and calculation, and possible sources of remaining discrepancies are discussed. The ^{37}Ar half-life is observed to be 35.02 ± 0.05 day, in good agreement with previously reported values.

[NUCLEAR REACTIONS $^{37}Cl(p,n)$, $E = 2$–24 MeV; measured $\sigma(E)$. Natural targets, Faraday cup, internal gas proportional counters. RADIOACTIVITY ^{37}Ar; measured $T_{1/2}$.]

I. INTRODUCTION

Numerous studies[1–14] of the $^{37}Cl(p,n)^{37}Ar$ reaction have been reported but only a few of these[1,5–9] deal directly with the excitation function. The energy range previously studied was from threshold (1.64 MeV) to only 5.5 MeV. Johnson and co-workers[5–7] used vacuum evaporated NaCl targets and 1.5–5.5-MeV protons from a Van de Graaff accelerator. The neutrons produced were counted with a 4π-flat-response graphite sphere detector. Barnard and co-workers[8,9] measured neutron yields from NaCl targets for (p,n) reactions to the ground state and to the first excited state of ^{37}Ar. They observed a large number of resonances in the $^{37}Cl(p,n)^{37}Ar$ cross section at proton energies up to 4 MeV. The present study was undertaken as part of an investigation in this laboratory of various (p,n) excitation functions.[15,16]

II. EXPERIMENTAL PROCEDURE

Thin NaCl targets (≈2 mg/cm^2) of natural isotopic abundances were made by vacuum deposition on 0.5-mm thick Al disks. The target thicknesses were determined by weighing and were checked in some cases by chemical analysis. The agreement between the two methods was better than 2%. The targets were enclosed in Al gas cells 2.5-cm diam, 2.0 cm deep, having 6.3-mg/cm^2 Havar windows. These cells were filled with air to a pressure of ≈200 Torr and then attached to a Faraday cup[15] for the proton bombardments. In addition, three other NaCl targets were sealed between Ag foils under vacuum in order to check the reliability of the ^{37}Ar recovery.

The Brookhaven tandem Van de Graaff accelerators were used as the sources of protons from 2.0 to 23.5 MeV. Average beam intensities were of the order of a few hundred nA and typical irradiation times were ≈30 min. Proton beams were magnetically analyzed with an energy resolution of ≤0.1%. The analyzed beam was diffused to minimize errors due to target nonuniformity and then collimated to a 1-cm-diam beam spot. The intensity was measured to an accuracy of <1% with a Faraday cup and current integrators which were calibrated against a standard current source.[15] The energy degradation of the beam in passing through various absorbers (aluminum window, air, Havar) and the target was calculated from the fitted[15] stopping power and range-energy data of Williamson, Boujot, and Picard,[17] and of Northcliffe and Schilling.[18] The energy of the proton beam midway through the NaCl target was taken as the energy of bombardment. The uncertainties in the mean energies, ≤25 keV, were obtained by quadratically propagating the uncertainties of the incident beam energies, of the energy losses for each absorber, and of the energy loss midway through the target. The target thicknesses varied from 32 keV at 23.5 MeV to 174 keV at 2.0 MeV. The effective energy resolution, which is obtained by quadratically summing the energy straggling[15] full width at half-maximum (FWHM) for each absorber and target thickness, ranged from 200 keV at the higher energy to 260 keV at the lower energy.

TABLE I. Experimental cross sections for the reaction $^{37}Cl(p,n)^{37}Ar$.

Proton energy [a] (MeV)	Cross section [b] (mb)	Proton energy [a] (MeV)	Cross section [b] (mb)
2.02	9.2	10.10	365
2.35	27.1	11.24	320
3.02	47.4	11.24	370
3.57	47.9	11.38	382 [c]
3.65	95.9	12.28	307
4.27	140	13.30	247
4.77	163	14.33	183
4.86	154	14.33	196
5.91	263	16.87	96.7
7.02	340	16.88	96.3
8.10	356	19.92	50.4
8.17	358 [c]	19.92	50.8
9.14	356	23.45	31.7
9.78	365 [c]	23.45	36.6

[a] Energy uncertainties are ≤25 keV, effective energy resolution varies from 260 keV at 2 MeV to 200 keV at 23.5 MeV.

[b] Estimated uncertainties of 6%.

[c] NaCl targets sealed in Ag foils; all other NaCl targets were enclosed in gas cells.

After irradiation each cell was attached to a vacuum system through a bellowed tube and ground glass joint. The ^{37}Ar in the gas phase and in the solid NaCl were separately purified and collected (see Appendix A). The radioactivity was assayed by transferring the Ar into cylindrical (1.9-cm i.d. and 30 cm long) Bernstein-Ballentine internal proportional counters.[19] The counting rate versus applied voltage exhibited distinct levels corresponding to the onset of K- and L-capture events. The counters were operated near the high voltage ends of the sum plateaus. The sensitive volume of these counters is equal to the cathode volume[20, 21] and was 82–84% of the total volume. The end effects for these counters were estimated to be <1% and the dead time ≃2 μsec.[21] The samples were assayed several times over periods of a few half-lives. The resultant decay curves were analyzed with the least-squares program CLSQ[22] to calculate the amount of ^{37}Ar activity at the end of bombardment. An accurate value of the half-life of ^{37}Ar was also obtained from CLSQ (see Appendix B). The disintegration rates obtained by applying the sensitive volume correction to the activities at the end of bombardment were used to determine reaction cross sections. The uncertainties in these values are ≈4% estimated from the propagation of errors (uncertainties in the thickness measurements 2%, in the beam intensities 1%, chemical recoveries 2%, counting efficiencies 1%, and counting statistics 1%). The error estimate based on the agreement of duplicate measurements is 6%. No significant differences were observed between the targets enclosed in gas cells and those sealed in Ag (see Table I).

III. RESULTS AND DISCUSSION

The experimental cross sections obtained in this measurement for the $^{37}Cl(p,n)^{37}Ar$ reaction are listed in Table I and shown in Fig. 1 as open circles. The excitation function is rather broad (FWHM ≈ 9.5 MeV) and the peak cross section is 365 mb at 10 MeV. The $^{37}Cl(p,n)^{37}Ar$ cross sections below 5 MeV are also plotted in Fig. 2 along with the data of Johnson, Galonsky, and Inskeep.[6] The agreement between the present set of measurements and their results is good except for one or two points. Figure 2 also shows the arbitrarily normalized sums of the neutron yields for the $^{37}Cl(p,n)^{37}Ar$ reactions to the ground state and to the first excited state taken from the measurements of Barnard, Mani, and Forsyth.[9] Their

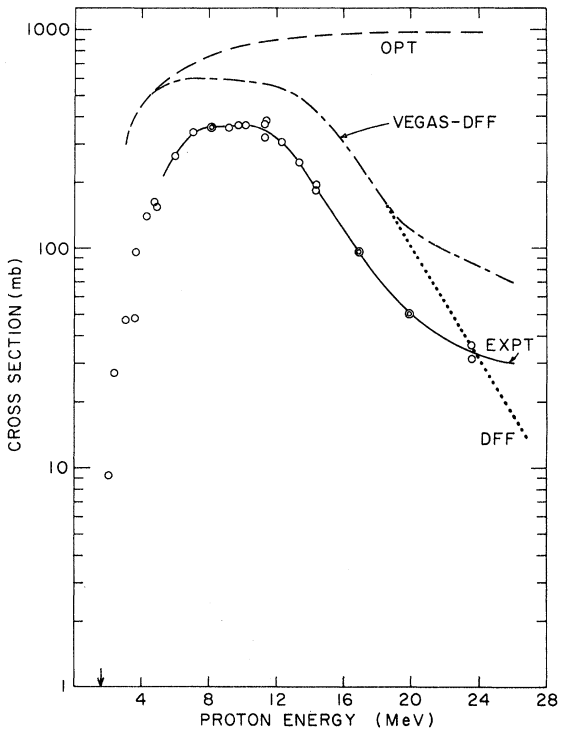

FIG. 1. Experimental and calculated excitation functions for the $^{37}Cl(p,n)^{37}Ar$ reaction. The circles represent the present measurements. The labeled curves are: EXPT, experimental; OPT, optical model reaction cross sections taken from Mani, Melkanoff, and Iori (Ref. 24); DFF, evaporation calculations; and VEGAS-DFF, cascade evaporation calculations for $r_0 = 1.5$ fm. The threshold for the $^{37}Cl(p,n)^{37}Ar$ reaction is shown by an arrow at 1.64 MeV.

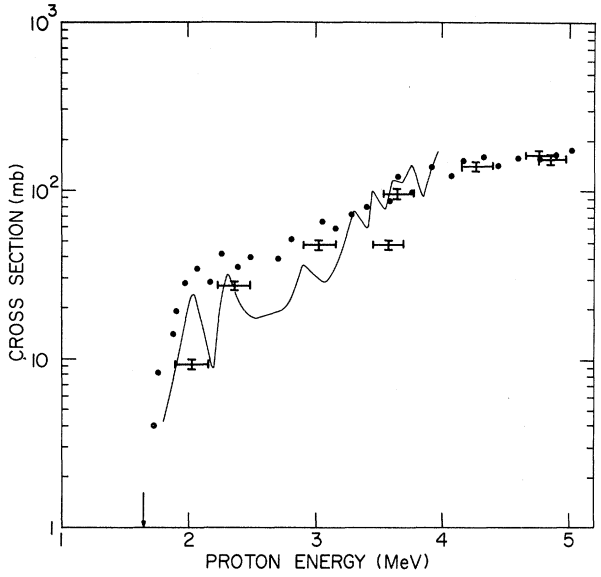

FIG. 2. Comparison of the present $^{37}Cl(p,n)^{37}Ar$ cross section measurements (⊢—⊣) with the measurements of Johnson, Galonsky, and Inskeep (Ref. 6) (filled circles) and with the arbitrarily normalized neutron yield measurements of Barnard, Mani, and Forsyth (Ref. 9) (solid curve). The horizontal bar width corresponds to effective energy resolution, and the vertical bar to an uncertainty of 6%. Target thicknesses: present measurements, 174 keV at 2 MeV; Johnson, Galonsky, and Inskeep, 115 keV at 3 MeV; Barnard, Mani, and Forsyth, ≈ 100 keV at 2 MeV.

target thickness was significantly thinner (≈100 keV at 2 MeV) than that used in the present work or by Johnson, Galonsky, and Inskeep[6] (115 keV at 3 MeV). The large fluctuations in the cross sections seen by Barnard *et al.* are expected to be damped in the present measurements. Our result at 3.57 MeV is probably low because of experimental error rather than a real fluctuation.

For comparison with the experimental data, two types of calculations were performed. In the first, cross sections for the (p,n) reaction over the entire energy region of interest were calculated using the DFF code of Dostrovsky, Fraenkel, and Friedlander[23] which treats particle evaporation from excited nuclei in terms of the statistical model. Fractional production probabilities given by DFF were converted to cross sections on the basis of the optical model total reaction cross sections of Mani, Melkanoff, and Iori[24] (MMI).

The second type of calculation, denoted VEGAS-DFF, employed the modified[25] STEPNO version of the VEGAS code of Chen *et al.*[26,27] to estimate the contribution of direct reaction and compound nuclear processes to (p,n) reactions at proton energies from 13 to 25 MeV. In this procedure, VEGAS gave the fractions of the inelastic cross section which led to compound nuclei and to the (p,n) product directly. Product formation via the compound nuclei was then calculated using DFF as above. It was observed that VEGAS-DFF and DFF gave essentially identical (p,n) cross sections at the peak of the excitation function[28] and thus we have used DFF for the calculations up to ≈12 MeV and VEGAS-DFF for the higher energies.

The dot-dashed curve labeled VEGAS-DFF in Fig. 1 is the $^{37}Cl(p,n)^{37}Ar$ excitation function calculated with the same nuclear radius and level density parameters ($r_0 = 1.5$ fm, $a = A/20$) which had been used in previous work from this laboratory.[15,16] However, pairing and shell correction energies (δ's) due to Hillman (MH)[29] were used because DFF[23] did not give δ values for the Cl-Ar region.

It is clear from Fig. 1 that the inclusion of direct reactions gives a better match to the shape

TABLE II. Comparison of experimental (p,n) cross sections at 10 MeV with those calculated using various parameter choices. (See text for detailed discussion.)

Target nucleus	Experimental (p,n) cross section (mb)	Optical model reaction cross sections MMI[a] (mb)	Perey[b] (mb)	BG[c] (mb)	Calculated (p,n) cross sections $r_0=1.5$ (mb)	$r_0=1.7$ (mb)	Effective Coulomb barrier $r_0=1.5$ (MeV)	$r_0=1.7$ (MeV)	Binding energy difference E_n-E_p (MeV)
^{37}Cl	365	845	882	994	566	506	2.60	1.94	1.49
^{63}Cu	410[d]	786	819	921	619	442	4.68	3.65	4.07
^{65}Cu	700[d]	792	849	969	768	707	4.64	3.61	2.10
^{79}Br	630[e]	725	805	899	713	675	5.52	4.35	2.37
^{107}Ag	595[d]	564	592	689	561	555	7.20	5.65	2.25
^{127}I	454[e]	500	519	614	500	500	7.85	6.10	1.74

[a] See Ref. 24.
[b] See Ref. 30.
[c] See Ref. 31.
[d] See Ref. 15.
[e] See Ref. 16.

of the tail of the excitation function for energies above 18 MeV. Cross sections calculated using the statistical model alone (shown as the dotted curve in the figure) decrease much too rapidly with energy. However, the VEGAS-DFF curve lies about a factor of 2 above the experimental values over the entire energy range.

To explore possible causes of this discrepancy and a similar one reported[15] in the case of ^{63}Cu-$(p,n)^{63}$Zn [but not for ^{65}Cu$(p,n)^{65}$Zn], calculations were performed at 10 MeV for six targets in which some of the input parameters were varied. The results are summarized in Table II.

Values of σ_R were obtained for three sets of optical model (OM) parameters. The cross sections in column 3 are from the tabulations of MMI.[24] Because of their convenience, the MMI tables had been used for the previous calculations[15,16] of (p,n) cross sections for ^{63}Cu, ^{65}Cu, ^{79}Br, ^{107}Ag, and ^{127}I. The values in columns 4 and 5 are based on the OM parameters deduced by Perey[30] and by Becchetti and Greenlees (BG),[31] respectively. They were calculated from the appropriate potentials and geometries by using the ABACUS-2 program of Auerbach.[32] The BG[31] cross sections are consistently larger than those of Perey,[30] which, in turn, are slightly higher than those of MMI.[24] Furthermore, the parameters of Perey or of BG give larger isotopic differences between ^{63}Cu and ^{65}Cu than do those of MMI. This is a consequence of the rather simple potentials used by MMI which did not include specific terms in $(N-Z)/A$.

It can be seen from Table II that the σ_R values from MMI and Perey are in good agreement with the experimental (p,n) cross sections for ^{107}Ag and ^{127}I given in column 2. For these heavy targets charged particle emission should be strongly suppressed at 10 MeV and the (p,n) cross section should closely approximate σ_R. On the other hand, the reaction cross sections from BG appear to be ≈20% too high. The authors had noted a similar effect at 14.5 MeV (see Fig. 5 of Ref. 31). As pointed out by Perey and Perey,[33] the derivation of the BG parameters was heavily weighted by elastic scattering data at 30 and 50 MeV. For the remaining calculations described below we have used the MMI values of σ_R.

Listed in columns 6 and 7 of Table II are (p,n) cross sections obtained from evaporation calculations for two choices of the nuclear radius parameter, $r_0 = 1.5$ fm and $r_0 = 1.7$ fm, $a = A/20$ and the MH δ set. As we shall see, the effect of increasing r_0 is to decrease the effective Coulomb barrier and, hence, to enhance the emission of charged particles. Use of the larger radius parameter appreciably improves the agreement with the experimental values. For targets from ^{63}Cu to ^{127}I, the calculated cross sections fall within 10% of those measured and the difference between the two copper isotopes is well reproduced. However, a 39% discrepancy remains for ^{37}Cl. Differences between the MH and DFF δ values appeared to have a small effect on the calculations. A comparison in the copper region where both sets were available gave 16% higher and 5% lower values for the ^{63}Cu$(p,n)^{63}$Zn and ^{65}Cu$(p,n)^{65}$Zn cross sections, respectively, when the DFF δ values were used compared with the entries for $r_0 = 1.5$ and the MH set in Table II. Changing the level density parameter from $a = A/20$ to $a = A/10$ gave slightly larger calculated cross sections (4% for both ^{63}Cu and ^{65}Cu and 14% for ^{37}Cl). In the calculations above, we have tried to apply single sets of OM parameters to data for a wide range of target systems. There is some question of whether such a "global" optical model is appropriate to a nucleus as light as ^{37}Cl.

The sensitivity of calculated cross sections to r_0 can be understood in terms of the role of the Coulomb barrier in determining inverse cross sections for charged particle emission. The DFF program approximates the cross section for proton capture σ_c as

$$\sigma_c/\sigma_g = (1+c_p)\left(1-\frac{k_p V_p}{\epsilon}\right), \tag{1}$$

where σ_g is the geometrical cross section and ϵ the proton energy. V_p is the classical Coulomb barrier,

$$V_p = \frac{zZe^2}{r_0 A^{1/3}}. \tag{2}$$

The parameters c_p and k_p are adjusted for each choice of r_0 to approximate the continuum theory barriers. It can be seen that $k_p V_p$ plays the role in Eq. (1) of an effective barrier below which protons cannot be emitted. Values of $k_p V_p$ used in the present calculations are also listed in Table II (column 8 for $r_0 = 1.5$ fm, column 9 for $r_0 = 1.7$ fm).

Provided $k_p V_p$ is at least a few MeV greater than the binding energy difference $E_n - E_p$, charged particle emission is strongly suppressed, and the calculated (p,n) cross section is nearly equal to the inelastic cross section; hence it is rather insensitive to changes in r_0. In these cases, ^{65}Cu, ^{79}Br, ^{107}Ag, and ^{127}I, the (p,n) cross sections at 10 MeV are calculated to an accuracy of ±10%.

It can be seen in Table II that the binding energy differences are comparable to the effective barriers for ^{37}Cl and ^{63}Cu. Charged particle emission competes favorably with neutron emission and the (p,n) cross section is sensitive to small changes in the parameters. It is interesting to note that

the changes in going from $a=A/20$ to $a=A/10$ can also be understood in terms of inverse cross sections. Increasing a lowers the nuclear temperature and softens the spectrum of emitted particles. When these are protons, their emission is suppressed by the barrier and the (p,n) cross section is increased. We believe an improved treatment of inverse cross sections is an essential step for more accurate calculations. However, until such calculations are available the use of $r_0=1.7$ and the Hillman δ set appears to give better agreement with experiment than does $r_0=1.5$ and the DFF δ's.[34]

As a summary, complete excitation functions were recalculated for the six (p,n) reactions using the VEGAS-DFF treatment and the better parameter set. In Fig. 3 these are shown as the dashed curves and the experimental data are shown as the solid curves. Agreement is significantly better than had been obtained with $r_0=1.5$ fm. The general overestimation for energies near 25 MeV probably arises from too large a contribution from direct processes in the STEPNO version of VEGAS in which refraction and reflection effects were ignored.

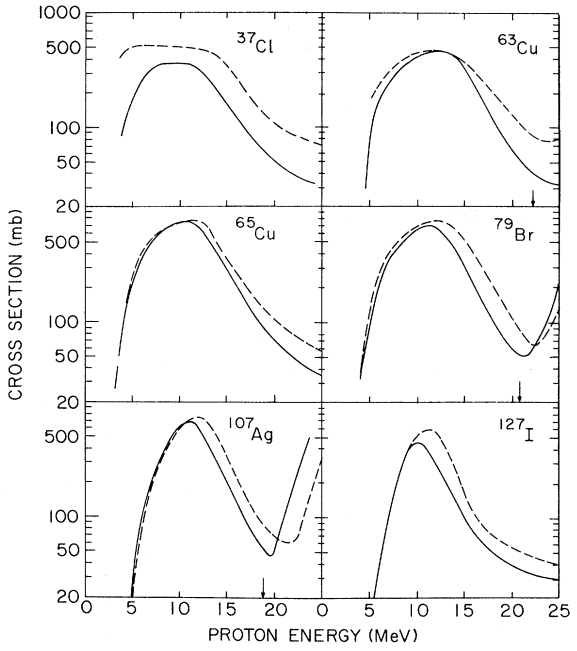

FIG. 3. Comparison of experimental excitation functions (solid curves) with the VEGAS-DFF cascade evaporation calculations (dashed curves) for the reactions: $^{37}Cl(p,n)^{37}Ar$ (present work), $^{63}Cu(p,n)^{63}Zn$ (Ref. 15), $^{65}Cu(p,n)^{65}Zn$ (Ref. 15), $^{79}Br(p,n)^{79}Kr$ (Ref. 16), $^{107}Ag(p,n)^{107}Cd$ (Ref. 15), and $^{127}I(p,n)^{127}Xe$ (Ref. 16). Parameters used: $r_0=1.7$ fm; $a=A/20$; Hillman δ values (Ref. 29).

ACKNOWLEDGMENTS

We are grateful to R. W. Stoenner for separating the ^{37}Ar from the NaCl targets sealed between Ag foils. Generous assistance was provided by E. Norton in performing the chlorine chemical analyses; E. Ritter, R. Becker, and R. Withnell in preparing the targets; E. Rowland and M. Kinney in punching cards for CLSQ analyses; and D. E. Alburger and the staff of the Brookhaven tandem Van de Graaff accelerator in obtaining proton irradiations. We thank G. D. Harp for help in carrying out the VEGAS and DFF calculations and for valuable discussions.

APPENDIX A

Several unforeseen problems were encountered in arriving at a suitable target configuration. The initial experiments were done with gaseous $CFCl_3$ (freon-11) targets in the gas cells at about 200 Torr pressure. It was noticed that certain gas cells always gave lower values of the cross sections than others. In those cells which gave low results, there was an appreciable decrease in pressure as a result of irradiation. A black deposit containing considerable chlorine was also observed in the cells after irradiation. All these facts suggested that some sort of catalytic polymerization of $CFCl_3$ was taking place during irradiation in some of the cells.

It was decided to use vacuum evaporated targets of NaCl which were encapsulated in vacuum between two sheets of $\simeq$12-mg/cm^2 heat-sealable Mylar, a technique developed for studies of the $^{79}Br(p,n)^{79}Kr$ and $^{127}I(p,n)^{127}Xe$ reactions.[16] After irradiation the ^{37}Ar was extracted from these targets by methods described previously[35] for Kr and Xe. The Mylar encapsulation was broken by heating the target after enclosing it in a glass bulb. Water was then admitted to the system to dissolve NaCl but the tar created by decomposing Mylar resulted in incomplete dissolution of NaCl. The results were found to be irreproducible because of the fact that 90% of ^{37}Ar is retained in NaCl grains and does not get completely removed until NaCl crystals are destroyed. This is contrary to the behavior of Kr and Xe which escape almost completely from KBr and KI targets.[35]

Finally, the present experimental arrangement was arrived at. In this, vacuum evaporated NaCl targets were enclosed in the gas cells for irradiation. After irradiation, the ^{37}Ar gas from the cell and from the NaCl targets were analyzed separately. A known amount of Ar carrier was added to the cell. After mixing the carrier and the activity the samples were transferred to hot ($\simeq$900°C)

TABLE III. Compilation of ^{37}Ar half-life measurements.

Authors	Reference	Half-life (day)
Weimer, Kurbatov, and Pool (1944)	36	34.1 ± 0.3
Miskel and Perlman (1952, 1953)	37	35.0 ± 0.4
Anderson, Wheeler, and Watson (1953)	38	32.0
Kiser and Johnston (1959)	39	34.30± 0.14
Stoenner, Schaeffer, and Katcoff (1965)	21	35.1 ± 0.1
Colomer and Gauvain (1973)	40	35.06± 0.18
Present work		35.02± 0.05

Ti getter, through a suitable system of cold traps, for about 20 min. After gettering, the chemical recovery was measured (losses were always less than 2%) and the gas samples were transferred into Bernstein-Ballentine proportional counters. The counters were then filled with P-10 counting gas (90% Ar and 10% CH_4) to a pressure of slightly above 1 atm. The NaCl targets were removed from the gas cells, placed in glass bulbs, evacuated, and a measured amount of Ar carrier was added. A few milliliters of dilute HCl and a few drops of Pd carrier were added to dissolve NaCl and part of the Al backing. The gasses were transferred to the hot Ti getter for about 20 min and the procedure was completed as described above.

The silver sealed targets were placed in molybdenum crucibles and a known amount of H_2-Ar mixture was added as carrier. Targets were evaporated by heating with an induction furnace to a temperature of 1300°C. The gases were gettered to purify the Ar which was then filled into the counters.

APPENDIX B

Various values for the ^{37}Ar half-life have been reported[21, 36-40] and are summarized in Table III. During the course of this work, numerous decay curves of ^{37}Ar (over one to three half-lives) were obtained. These data were analyzed by the least squares analysis program CLSQ of Cumming.[22] The weighted mean value (inverse square of the standard deviations) based on 28 measurements is 35.02 ± 0.02 day, where the uncertainty is one standard deviation σ. The goodness-of-fit parameter[41] $\hat{\sigma}$ is 1.013. If the error is increased to reflect a 99% confidence limit, the value of the ^{37}Ar half-life obtained is 35.02 ± 0.05 day which is in very good agreement with three of the previously reported values but not with some of the older values.

*Research supported by the Advanced Research Projects Agency (ARPA order No. 1590) and the U.S. Energy Research and Development Administration.

†Present address: Department of Nuclear Medicine, Veterans Administration Hospital, Albany, New York 12208.

‡Present address: Radiation Physics C114, National Bureau of Standards, Washington, D. C. 20234.

[1]J. P. Blaser, F. Boehm, P. Marmier, and P. Scherrer, Helv. Phys. Acta 24, 30 (1951).

[2]K. J. Brostrøm, B. S. Madsen, and C. B. Madsen, Phys. Rev. 83, 1265 (1951).

[3]W. A. Schoenfeld, R. W. Duborg, W. M. Preston, and C. Goodman, Phys. Rev. 85, 873 (1952).

[4]P. H. Stelson and W. M. Preston, Phys. Rev. 86, 807 (1952).

[5]C. H. Johnson, A. Galonsky, and J. P. Ulrich, Phys. Rev. 109, 1243 (1958).

[6]C. H. Johnson, A. Galonsky, and C. N. Inskeep, Progress Report, February 10, 1960, Oak Ridge National Laboratory Report No. ORNL-2910 (unpublished).

[7]C. H. Johnson (private communication).

[8]G. S. Mani, A. C. L. Barnard, T. A. Tombrello, and D. A. A. S. N. Rao, Nucl. Phys. 28, 456 (1961).

[9]A. C. L. Barnard, G. S. Mani, and P. D. Forsyth, Nucl. Phys. 28, 464 (1961).

[10]K. V. K. Iyengar, S. K. Gupta, B. Lal, and E. Kondaiah, Nucl. Phys. 76, 433 (1966).

[11]P. B. Parks, P. M. Beard, E. G. Bilpuch, and H. W. Newson, Nucl. Phys, 85, 504 (1966).

[12]S. K. Gupta, S. S. Kerekatte, and A. S. Divatia, in Proceedings of the Nuclear Physics and Solid State Physics Symposium, Roorkee, 1969 (unpublished).

[13]P. Taras, A. Turcotte, R. Vaillancourt, and J. Matas, Can. J. Phys. 49, 1215 (1971).

[14]P. Taras, A. Turcotte, and R. Vaillancourt, Can. J. Phys. 50, 1182 (1972).

[15]R. Collé, R. Kishore, and J. B. Cumming, Phys. Rev. C 9, 1819 (1974).

[16]R. Collé and R. Kishore, Phys. Rev. C 9, 2166 (1974).

[17]C. F. Williamson, J. P. Boujot, and J. Picard, Centre d'Études Nucléaires de Saclay Report No. CEA-R3042,

1966 (unpublished).
[18]L. C. Northcliffe and R. F. Schilling, Nucl. Data A7, 223 (1970).
[19]W. Bernstein and R. Ballentine, Rev. Sci. Instrum. 21, 158 (1950).
[20]S. Katcoff, Phys. Rev. 87, 886 (1952).
[21]R. W. Stoenner, O. A. Schaeffer, and S. Katcoff, Science 148, 1325 (1965).
[22]J. B. Cumming, National Academy of Sciences, National Research Council, Nuclear Science Series Report No. NAS NS-3107, 1962 (unpublished).
[23]I. Dostrovsky, Z. Fraenkel, and G. Friedlander, Phys. Rev. 116, 683 (1959).
[24]G. S. Mani, M. A. Melkanoff, and I. Iori, Centre d'Études Nucléaires de Saclay Report No. CEA-2379, 1963 (unpublished).
[25]The calculation employed an improved nucleon density distribution as discussed by K. Chen, G. Friedlander, and J. M. Miller, Phys. Rev. 176, 1208 (1968).
[26]K. Chen, Z. Fraenkel, G. Friedlander, J. R. Grover, J. M. Miller, and Y. Shimamoto, Phys. Rev. 166, 949 (1968).
[27]K. Chen, G. Friedlander, G. D. Harp, and J. M. Miller, Phys. Rev. C 4, 2234 (1971).
[28]It is interesting to note that for energies of ≈ 14 MeV the VEGAS-DFF calculation predicts a somewhat smaller (p,n) cross section that the pure DFF calculation. This is a consequence of (p,p') and (p,n) cascades which do not lead to the product but do subtract from the total reaction cross section.
[29]M. Hillman (unpublished). His values for δ were derived from mass data. Those relevant to the present work are tabulated below. For $Z=30$ and $N=34, 36$ δ values derived by DFF (Ref. 23) are given in parentheses.

Z	δ (MeV)	N	δ (MeV)
18	1.524	20	2.056
30	0.736(0.50)	34	1.262(1.90)
		36	1.464(0.50)
36	1.190	44	1.389
48	1.333	60	1.093
54	1.101	74	1.449

[30]F. G. Perey, Phys. Rev. 131, 745 (1963).
[31]F. D. Becchetti, Jr., and G. W. Greenlees, Phys. Rev. 182, 1190 (1969).
[32]E. Auerbach (unpublished).
[33]C. M. Perey and F. G. Perey, At. Nucl. Data Tables 13, 293 (1974).
[34]This is similar to the conclusion drawn by DFF in footnote 45 of Ref. 26.
[35]R. Collé and R. Kishore, Phys. Rev. C 9, 981 (1974).
[36]P. K. Weimer, J. D. Kurbatov, and M. L. Pool, Phys. Rev. 66, 209 (1944).
[37]J. A. Miskel and M. L. Perlman, Phys. Rev. 87, 543 (1952); M. L. Perlman and J. A. Miskel, *ibid.* 91, 899 (1953).
[38]C. E. Anderson, G. W. Wheeler, and W. W. Watson, Phys. Rev. 90, 606 (1953).
[39]R. W. Kiser and W. H. Johnston, J. Am. Chem. Soc. 81, 1810 (1959).
[40]J. Colomer and D. Gauvain, Int. J. Appl. Radiat. Isot. 24, 391 (1973).
[41]The goodness-of-fit parameter ($\hat{\sigma}$) is given by the square root of the weighted sum of the residuals divided by the degrees of freedom (ν), i.e.,

$$\hat{\sigma}=\left[\left(\sum_i(\bar{x}-x_i)^2/\sigma_i^2\right)\Big/\nu\right]^{1/2};$$

cf. W. C. Hamilton, *Statistics of Physical Science* (Ronald Press, New York, 1964), p. 130.